Periodically Driving a Many-Body Localized Quantum System

Pranjal Bordia,[1,2] Henrik Lüschen,[1,2] Ulrich Schneider,[1,2,3] Michael Knap,[4] and Immanuel Bloch[1,2]

[1] *Fakultät für Physik, Ludwig-Maximillians-Universität München, Schellingstr. 4, 80799 Munich, Germany*
[2] *Max-Planck-Institut für Quantenoptik, Hans-Kopfermann-Str. 1, 85748 Garching, Germany*
[3] *Cavendish Laboratory, University of Cambridge, J.J. Thomson Avenue, Cambridge CB3 0HE, United Kingdom*
[4] *Department of Physics, Walter Schottky Institute, and Institute for Advanced Study, Technical University of Munich, 85748 Garching, Germany*

(Dated: December 11, 2016)

Quantum many-body systems far from equilibrium arise naturally in a variety of disciplines, ranging from condensed matter to cosmology. In recent years, there has been an intense focus on understanding the dynamical evolution of quantum many-body systems that are well isolated from their environment [1, 2]. Particularly, in periodically driven systems exotic phenomena can emerge that are absent in their undriven counterparts. For example, topologically non-trivial band structures can be realized by driving topologically trivial systems [3–9] and ergodic phases can be created by driving non-ergodic quantum systems [10–16]. In undriven systems, a robust *non-ergodic* phase can be realized by adding strong disorder to an interacting many-body system, leading to the phenomenon of many-body localization (MBL) [17–25]. In an ideal MBL phase, global transport and thermalization are absent, and some memory of the initial conditions persists locally for arbitrarily long times even at finite energy densities [19, 20], as underlined in experiments [22–25]. Recent theoretical works have further proposed that combining MBL and periodic driving can lead to novel symmetry protected topological phases with no direct equilibrium analogues [26–32]. It is therefore highly pertinent to experimentally study the interplay of disorder and periodic driving in interacting quantum systems.

In this work, we experimentally study a periodically modulated, disordered many-body system by employing an interacting Fermi gas in a one-dimensional quasi-random optical lattice. The undriven system exhibits a phase transition from an ergodic to an MBL phase as the disorder strength is increased [22]. In presence of a strong drive, we observe a stable MBL phase at high drive frequencies, characterized by a persisting memory on the initial state for long times. In contrast, below a critical frequency, the system delocalizes and completely obliviates the initially imprinted density modulation, see Fig. 1. These phases are separated by a dynamical phase transition that depends on both the drive amplitude and the frequency. Our observations are supported by numerical simulations based on matrix product states and exact diagonalization and can be understood as emergent properties of an effective Floquet Hamiltonian.

Experiment.— Our experimental setup consists of a degenerate ^{40}K Fermi gas prepared in an equal spin mixture of its lowest two hyperfine states, denoted as $\{\uparrow,\downarrow\}$. We load the gas into the lowest band of a deep three-dimensional optical lattice with at most one atom per site. In the x-direction, we employ a superlattice [22] to imprint a density modulation with atoms occupying only even sites of the primary lattice, Fig. 1 (a). We initiate the quantum dynamics by lowering the depth of the longitudinal lattice, so that quantum tunneling becomes appreciable along one direction and the density pattern coherently evolves in a one-dimensional quasi-random disorder potential. This quasi-random potential is generated by superimposing a primary lattice beam of wavelength $\lambda_s = 532.0\,\mathrm{nm}$ with a second laser, the disorder lattice laser, of incommensurate wavelength $\lambda_d = 738.2\,\mathrm{nm}$. During the time evolution, we continuously modulate all on-site potentials Δ_i synchronously by modulating the disorder lattice intensity with frequency ν, Fig. 1 (b). After a variable evolution time, we suddenly freeze the system by increasing the depth of the primary lattice and thereby suppressing tunneling. Subsequently, we employ a bandmapping procedure to measure the particle number on even N_e and odd N_o sites in time-of-flight images [22] and calculate the imbalance $\mathcal{I} = (N_e - N_o)/(N_e + N_o)$, which effectively provides a measure for the ergodicity of the quantum system: Under ergodic evolution it rapidly approaches zero while a persistent imbalance indicates non-ergodic dynamics.

Model.— Our system can be described theoretically by the one-dimensional Aubry-André model with on-site interactions [33] and a time periodic quasi-random disorder potential:

$$\hat{H} = -J\sum_{i,\sigma}(\hat{c}^{\dagger}_{i+1,\sigma}\hat{c}_{i,\sigma} + \mathrm{h.c.}) + U\sum_{i}\hat{n}_{i,\uparrow}\hat{n}_{i,\downarrow} + [\Delta + A\sin(2\pi\nu t)]\sum_{i,\sigma}\cos(2\pi\beta i + \phi)\hat{n}_{i,\sigma}. \quad (1)$$

Here, $J \approx h \times 550\,\mathrm{Hz}$ is the tunneling matrix element between neighboring sites and h is the Planck's constant.

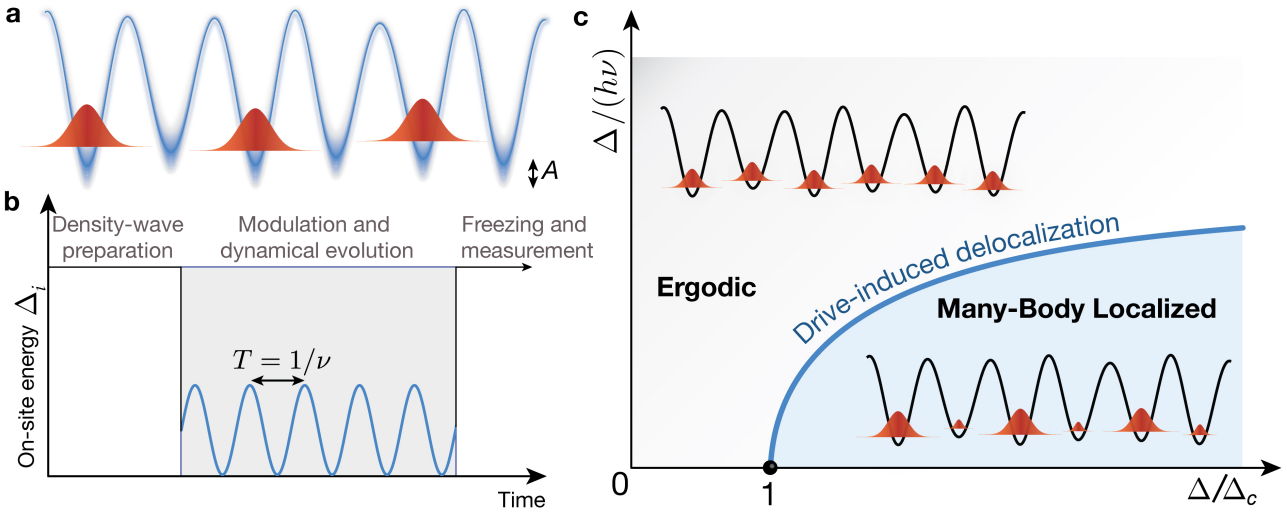

FIG. 1. **Schematic of the experiment and the dynamical phase diagram.** **(a)** A density-wave pattern of spinful fermionic atoms occupying only the even sites of a disordered optical lattice evolves under **(b)** a periodic modulation of the on-site disorder potentials Δ_i with frequency ν and amplitude A. **(c)** The phase diagram for the strongly driven system ($A = \Delta$) as a function of inverse frequency $1/\nu$ and characteristic disorder strength Δ: In the infinite-frequency limit (x-axis), the *disorder-induced* phase transition from an ergodic phase to a many-body localized phase is recovered at a critical disorder strength Δ_c (black point). While at high but finite drive frequencies the system remains localized for strong disorder, it delocalizes at low drive frequencies. These phases are separated by a *drive-induced* transition (blue line).

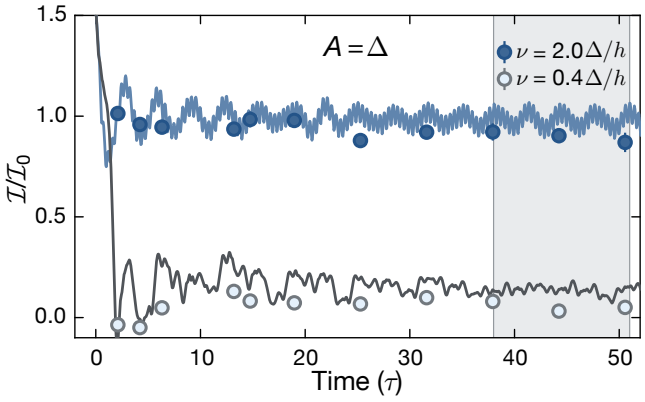

FIG. 2. **Evolution of the imbalance under periodic modulation.** The initially imprinted density-wave pattern, in which atoms occupy only even sites, evolves in a quasi-random disorder potential that is periodically modulated in time. After variable evolution times, we measure the imbalance between the even and odd sites. Fixing the disorder $\Delta = 7.5\,J$ and interaction strength $U = 4\,J$, experimental data (symbols) and numerical simulations (lines) are shown for different values of the drive frequency ν (legend), for the strongly driven case with $A = \Delta$. Experimental and numerical data are normalized by their respective asymptotic values in the undriven system $\mathcal{I}_0 \approx 0.6$. The experimental data is averaged over six different disorder realizations and the error-of-the-mean (e.o.m) is smaller than the symbol size. The light gray area indicates the time window considered to determine the asymptotic imbalance. Theoretical data to longer times is shown in the Supplementary Material.

The fermion creation (annihilation) operator in the spin state $\sigma \in \{\uparrow, \downarrow\}$ on site i are denoted by $\hat{c}^\dagger_{i,\sigma}$ ($\hat{c}_{i,\sigma}$) and the particle number operator is $\hat{n}_{i,\sigma} = \hat{c}^\dagger_{i,\sigma}\hat{c}_{i,\sigma}$. The on-site interaction strength between the two spin species is given by U. The disorder is characterized by the disorder strength Δ, the incommensurate wavelength ratio $\beta = \lambda_s/\lambda_d$, and the relative phase ϕ.

The disorder is modulated in time with frequency ν and amplitude $A \in [0, \Delta]$, Fig. 1 (b). The total Hamiltonian is thus periodic in time $H(t) = H(t+T)$ with period $T = 1/\nu$. For $A = 0$ the model has been experimentally shown to exhibit an MBL phase above a critical disorder strength Δ_c for a wide range of interactions and energy densities [22].

Dynamic Response.— First, we concentrate on fixed disorder $\Delta = 7.5\,J$ and interactions $U = 4\,J$. For these parameters, the undriven system ($A = 0$) is deep in the localized phase and an initial density-wave pattern approaches a stationary state with large residual imbalance $\mathcal{I}_0 \approx 0.6$ (see Supplementary Material). The time evolution of the normalized imbalance $\mathcal{I}/\mathcal{I}_0$ for the strongly driven system $A = \Delta$ is shown in Fig. 2 for two different drive frequencies. All times are given in units of tunneling time, $\tau = h/(2\pi J)$. At high drive frequency $\nu = 2\,\Delta/h$ the system remains localized ($\mathcal{I}/\mathcal{I}_0 \sim 1$), implying that the system is transparent to the drive in this regime. In this case, its dynamics is effectively governed by the time averaged non-ergodic Hamiltonian. By contrast, at low drive frequency $\nu = 0.4\,\Delta/h$, the drive enables a redistribution of atoms leading to a vanish-

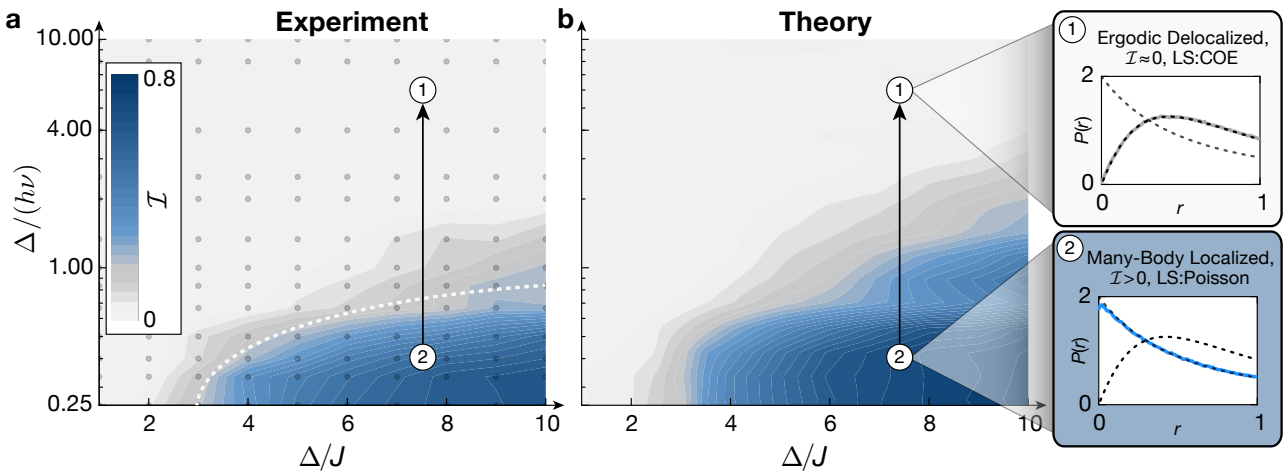

FIG. 3. **Dynamical phase diagram.** Asymptotic imbalance, $\mathcal{I}$, as a function of the disorder strength Δ/J and inverse frequency Δ/ν for strong drive $A = \Delta$ and interactions $U = 4\,J$. **(a)** The interpolated experimental measurements (data taken at the gray dots), are compared to **(b)** numerical simulations based on matrix product states. We find a drive-induced delocalization transition (white dashed line, guide to the eye) from the many-body localized phase with high imbalance (blue) to an ergodic phase with vanishing imbalance (gray) when lowering the drive frequency. Using exact diagonalization, the drive induced delocalization transition is also supported by the quasienergy level statistics of the Floquet Hamiltonian, insets to the right. The distribution $P(r)$ of the level statistics parameter r (see main text) follows the circular orthogonal ensemble (COE) in the ergodic phase (gray curve, ①) and Poisson statistics in the localized phase (blue curve, ②). In both insets, the dashed black lines indicate the Poisson and COE distribution functions, respectively.

ingly small imbalance ($\mathcal{I}/\mathcal{I}_0 \sim 0$). Thus, the dynamics is consistent with ergodic behavior, even though the time-averaged Hamiltonian is not. The theoretical data (solid lines), obtained by numerical simulations based on matrix product states, agrees with the experimental measurements (symbols), Fig. 2, and provides strong support for the observed behavior. Furthermore, the good agreement indicates that the system is minimally affected from any external couplings on the experimental time scales [24, 34].

Phase Diagram.— To investigate the dynamical phases, we systematically study the long-time asymptotics of the imbalance in the strongly driven system. We measure the asymptotic imbalance $\mathcal{I}$ as the time average between $\sim 40\,\tau - 50\,\tau$, as marked by the light-gray area in Fig. 2. The experimentally measured and theoretically calculated mean imbalance for strong drive $A = \Delta$ and interactions $U = 4\,J$ is shown in Fig. 3 as a function of drive frequency and disorder strength. We note that in this regime, the system is far away from the weak driving considered in linear response. The x-axis marks the limit of infinite drive frequency $\Delta/(h\nu) \to 0$, where the imbalance reduces to the one of the undriven system and connects to the phase diagram measured in Ref. [22].

We observe a stable MBL phase at high but finite frequencies, which is illustrated by the blue area in Fig. 3. When lowering the drive frequency at fixed disorder strength and drive amplitude the system undergoes a delocalization transition to the ergodic phase (② to ①, black arrow). We emphasize that, due to the sinusoidal drive, the fraction of time spent by the system in the delocalized regime is *independent* of the drive frequency. Yet, the nature of the effective dynamics changes completely with its frequency. This arises because at high drive frequencies the atoms only respond to the time-averaged on-site potential, while at low frequencies they can delocalize via the intermediate extended states. The two phases are separated by a *drive* induced delocalization transition. This phase boundary is indicated by the white dashed line (guide to the eye) in Fig. 3 (a), which follows the contour line connecting to the approximate critical disorder strength $\Delta_c \approx 3\,J$ in the infinite frequency limit (x-axis in Fig. 3 (c)) [22].

For the theoretical interpretation of the observed drive-induced phase transition, it is useful to introduce the Floquet Hamiltonian $\hat{H}_F$ as

$$e^{-\frac{i}{\hbar}\hat{H}_F T} = \mathcal{T} e^{-\frac{i}{\hbar}\int_0^T \hat{H}(t)dt} \tag{2}$$

which describes the unitary evolution over one period of the drive. Here, $\mathcal{T}$ is the time ordering operator and $\hbar$ is the reduced Planck's constant. The Floquet Hamiltonian governs the stroboscopic dynamics of the system and its statistical properties determine whether the quantum dynamics is ergodic or not [35]. This can be exemplified by studying the level statistics of the quasienergies ϵ_α obtained from diagonalizing $\hat{H}_F$. Due to the periodic drive, the quasienergies ϵ_α are only defined modulo h/T. The distribution $P(r)$ of the level statistics parameter $r_\alpha = \min[\frac{\epsilon_{\alpha+1}-\epsilon_\alpha}{\epsilon_\alpha-\epsilon_{\alpha-1}}, \frac{\epsilon_\alpha-\epsilon_{\alpha-1}}{\epsilon_{\alpha+1}-\epsilon_\alpha}]$ enables one to identify the nature of the phases [19]. While an ergodic system

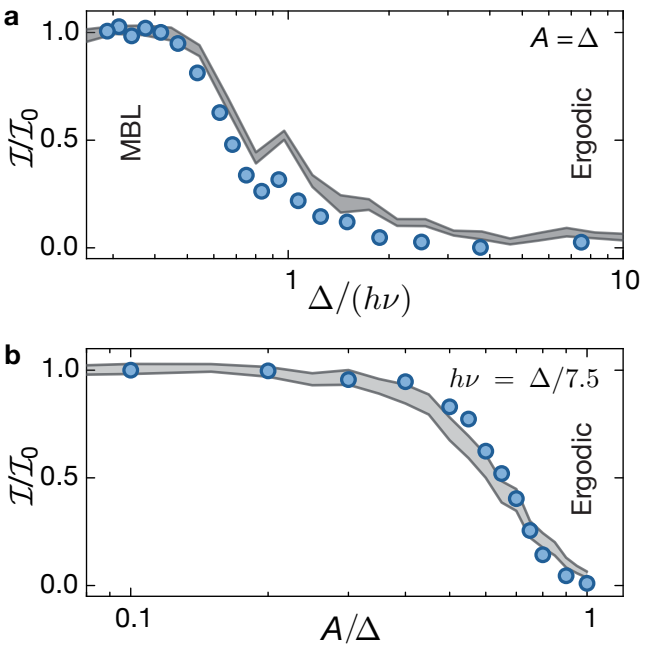

FIG. 4. **Frequency and amplitude dependence of the asymptotic imbalance.** We choose disorder $\Delta = 7.5\,J$ and interaction $U = 3\,J$ for which the undriven system is strongly localized. **(a)** The measured (symbols) and numerical (gray shaded area) data of the asymptotic normalized imbalance $\mathcal{I}/\mathcal{I}_0$ is shown as a function of inverse drive frequency $\Delta/(h\nu)$ for strong drive amplitude $A = \Delta$. **(b)** Asymptotic imbalance as a function of drive amplitude A/Δ for comparatively low drive frequency $h\nu = \Delta/7.5$. The system appears to remain exceedingly stable at low amplitudes but promptly delocalizes for larger amplitudes. E.o.m. over six disorder realizations is smaller than the symbol size. Thickness of the theoretical lines denote one standard deviation of the data for different disorder configurations.

is expected to follow the circular orthogonal ensemble, a Poisson distribution is expected in the localized phase due to the absence of level repulsion [19, 35]. Typical plots for the distribution $P(r)$ are shown in the insets in Fig. 3 and agree with these expectations. To keep the numerical computation of the level statistics tractable, we have approximated the monochromatic drive by a two-step function (see Supplementary Material for further details).

Quantitative Analysis of Frequency and Amplitude Dependence.— In order to quantitatively study the frequency dependence of the imbalance for a strong amplitude drive $A = \Delta$, we choose disorder $\Delta = 7.5\,J$ and interactions $U = 3\,J$ and illustrate in Fig. 4 (a) the transition from the localized phase at high frequencies to the ergodic phase at low ones. The imbalance decreases continuously with decreasing frequency except for a small peak around $\Delta/(h\nu) \approx 1$, a fact which is also discernible in theoretical contours in Fig. 3 and stems from the energy level distribution of the quasi-periodic disorder potential (see Supplementary Material for further details). At low frequencies with $\Delta/(h\nu) \gtrsim 2$, we measure close to vanishing imbalances consistent with ergodic dynamics. In this regime, small residual imbalance in the theoretical simulations follows a slow power law relaxation (see Supplementary Material). Due to the finite lifetime in the experiment, the theoretically evaluated imbalance is typically slightly larger than the experimental one [24].

The response of the system as a function of the drive amplitude at *low drive frequency* $h\nu = \Delta/7.5$ is shown in Fig. 4 (b). The normalized imbalance decreases as a function of the drive amplitude and for strong drives ($A \approx \Delta$), the system delocalizes with vanishing steady state imbalance. Crucially, despite the comparatively low drive frequency, the system remains *exceedingly stable* for drive amplitudes that are small compared to the disorder strength. The stability of the MBL phase at such low frequencies is a consequence of the drive modulating all on-site energies synchronously, i.e., modulating the overall disorder strength itself. This is in contrast to previous theoretical studies in which a linear-field gradient drive was used. For such a drive, similar parameters would already result in delocalization through a series of Landau-Zener transitions [13, 16]. For our case, we cannot rule out delocalization at even longer times or lower drive frequencies. In particular, the critical drive frequency below which the system might delocalize could get reduced to extremely small values. Analyzing these extreme limits remains a challenging task for future work.

Nonetheless, we find an exceptionally stable driven phase even at low drive frequencies that can provide novel avenues for engineering exotic phases of matter [26–32]. In the Supplementary Material, we also present the dynamical phase diagram as a function of the amplitude and frequency.

Conclusions and Outlook.— By periodically driving a many-body localized system, we have created and observed non-ergodic and ergodic phases that emerge from an effective Floquet Hamiltonian and are separated by a drive-induced delocalization transition. Our results directly show dynamics beyond the time-averaged Hamiltonian. Periodic modulation paves the way for measuring the frequency resolved response of many-body systems, with the particular prospect of exploring the critical point of the MBL transition [36–39] and the response in higher dimensions [25]. Furthermore, our observations demonstrate that disorder can be used to protect interacting and periodically driven systems from heating to infinite temperature and hence sets the basis for realizing novel symmetry protected topological phases [26–32].

Acknowledgments.— We thank E. Altman, E. Demler, S. Gopalakrishnan, and S. Hodgman for many useful discussions. We acknowledge support from Technical University of Munich - Institute for Advanced Study, funded by the German Excellence Initiative and the European Union FP7 under grant agreement 291763, from

the DFG grant No. KN 1254/1-1, the European Commission (UQUAM, AQuS) and the Nanosystems Initiative Munich(NIM).

Material and Data Request.— Correspondence should be addressed to I. Bloch (immanuel.bloch@mpq.mpg.de). The data that support the plots within this paper and other findings are available from the corresponding author upon reasonable request.

[1] I. Bloch, J. Dalibard, and W. Zwerger, "Many-body physics with ultracold gases," Rev. Mod. Phys. **80**, 885–80 (2008).

[2] A. Polkovnikov, K. Sengupta, A. Silva, and M. Vengalattore, "Colloquium: Nonequilibrium dynamics of closed interacting quantum systems," Rev. Mod. Phys. **83**, 863–883 (2011).

[3] T. Oka and H. Aoki, "Photovoltaic hall effect in graphene," Phys. Rev. B **79**, 081406 (2009).

[4] T. Kitagawa, E. Berg, M. Rudner, and E. Demler, "Topological characterization of periodically driven quantum systems," Phys. Rev. B **82**, 235114 (2010).

[5] N. H. Lindner, G. Refael, and V. Galitski, "Floquet topological insulator in semiconductor quantum wells," Nat. Phys. **7**, 490–495 (2011).

[6] M. Aidelsburger, M. Atala, M. Lohse, et al., "Realization of the hofstadter hamiltonian with ultracold atoms in optical lattices," Phys. Rev. Lett. **111**, 185301 (2013).

[7] H. Miyake, G. A. Siviloglou, C. J. Kennedy, W. C. Burton, and W. Ketterle, "Realizing the harper hamiltonian with laser-assisted tunneling in optical lattices," Phys. Rev. Lett. **111**, 185302 (2013).

[8] G. Jotzu, M. Messer, R. Desbuquois, et al., "Experimental realization of the topological haldane model with ultracold fermions," Nature **515**, 237–240 (2014).

[9] M. Aidelsburger, M. Lohse, C. Schweizer, et al., "Measuring the chern number of hofstadter bands with ultracold bosonic atoms," Nat. Phys. **11**, 162–166 (2015).

[10] P. Ponte, A. Chandran, Z. Papić, and D. A. Abanin, "Periodically driven ergodic and many-body localized quantum systems," Ann. Phys. **353**, 196–204 (2015).

[11] P. Ponte, Z. Papić, F. Huveneers, and D. A. Abanin, "Many-body localization in periodically driven systems," Phys. Rev. Lett. **114**, 140401 (2015).

[12] A. Lazarides, A. Das, and R. Moessner, "Fate of many-body localization under periodic driving," Phys. Rev. Lett. **115**, 030402 (2015).

[13] D. A. Abanin, W. D. Roeck, and Francois, "Theory of many-body localization in periodically driven systems," Ann. Phys. **372**, 1 – 11 (2016).

[14] M. Kozarzewski, P. Prelovšek, and M. Mierzejewski, "Distinctive response of many-body localized systems to a strong electric field," Phys. Rev. B **93**, 235151 (2016).

[15] J. Rehn, A. Lazarides, F. Pollmann, and R. Moessner, "How periodic driving heats a disordered quantum spin chain," Phys. Rev. B **94**, 020201 (2016).

[16] S. Gopalakrishnan, M. Knap, and E. Demler, "Regimes of heating and dynamical response in driven many-body localized systems," Phys. Rev. B **94**, 094201 (2016).

[17] P. W. Anderson, "Absence of diffusion in certain random lattices," Phys. Rev. **109**, 1492–1505 (1958).

[18] D. Basko, I. Aleiner, and B. Altshuler, "Metal-insulator transition in a weakly interacting many-electron system with localized single-particle states," Ann. Phys. **321**, 1126 – 1205 (2006).

[19] R. Nandkishore and D. A. Huse, "Many-body localization and thermalization in quantum statistical mechanics," Annu. Rev. Condens. Matter Phys. **6**, 15–38 (2015).

[20] E. Altman and R. Vosk, "Universal dynamics and renormalization in many-body-localized systems," Annu. Rev. Condens. Matter Phys. **6**, 383–409 (2015).

[21] S. S. Kondov, W. R. McGehee, W. Xu, and B. DeMarco, "Disorder-induced localization in a strongly correlated atomic hubbard gas," Phys. Rev. Lett. **114**, 083002 (2015).

[22] M. Schreiber, S. S. Hodgman, P. Bordia, et al., "Observation of many-body localization of interacting fermions in a quasirandom optical lattice," Science **349**, 842–845 (2015).

[23] J. Smith, A. Lee, P. Richerme, et al., "Many-body localization in a quantum simulator with programmable random disorder," Nat. Phys. **12**, 907–911 (2016).

[24] P. Bordia, H. P. Lüschen, S. S. Hodgman, et al., "Coupling identical one-dimensional many-body localized systems," Phys. Rev. Lett. **116**, 140401 (2016).

[25] J.-y. Choi, S. Hild, J. Zeiher, et al., "Exploring the many-body localization transition in two dimensions," Science **352**, 1547–1552 (2016).

[26] V. Khemani, A. Lazarides, R. Moessner, and S. L. Sondhi, "Phase structure of driven quantum systems," Phys. Rev. Lett. **116**, 250401 (2016).

[27] D. V. Else and C. Nayak, "Classification of topological phases in periodically driven interacting systems," Phys. Rev. B **93**, 201103 (2016).

[28] C. W. von Keyserlingk and S. L. Sondhi, "Phase structure of one-dimensional interacting floquet systems. i. abelian symmetry-protected topological phases," Phys. Rev. B **93**, 245145 (2016).

[29] C. W. von Keyserlingk and S. L. Sondhi, "Phase structure of one-dimensional interacting floquet systems. ii. symmetry-broken phases," Phys. Rev. B **93**, 245146 (2016).

[30] A. C. Potter, T. Morimoto, and A. Vishwanath, "Classification of interacting topological floquet phases in one dimension," Phys. Rev. X **6**, 041001 (2016).

[31] D. V. Else, B. Bauer, and C. Nayak, "Floquet time crystals," Phys. Rev. Lett. **117**, 090402 (2016).

[32] C. W. von Keyserlingk, V. Khemani, and S. L. Sondhi, "Absolute stability and spatiotemporal long-range order in floquet systems," Phys. Rev. B **94**, 085112 (2016).

[33] S. Iyer, V. Oganesyan, G. Refael, and D. A. Huse, "Many-body localization in a quasiperiodic system," Phys. Rev. B **87**, 134202 (2013).

[34] H. P. Lüschen, P. Bordia, S. S. Hodgman, et al., "Signatures of many-body localization in a controlled open quantum system," arXiv:1610.01613 (2016).

[35] L. D'Alessio and M. Rigol, "Long-time behavior of isolated periodically driven interacting lattice systems," Phys. Rev. X **4**, 041048 (2014).

[36] K. Agarwal, S. Gopalakrishnan, M. Knap, M. Müller, and E. Demler, "Anomalous diffusion and griffiths effects near the many-body localization transition," Phys. Rev. Lett. **114**, 160401 (2015).

[37] R. Vosk, D. A. Huse, and E. Altman, "Theory of the many-body localization transition in one-dimensional systems," Phys. Rev. X **5**, 031032 (2015).

[38] A. C. Potter, R. Vasseur, and S. A. Parameswaran, "Universal properties of many-body delocalization transitions," Phys. Rev. X **5**, 031033 (2015).

[39] S. Gopalakrishnan, M. Müller, V. Khemani, et al., "Low-frequency conductivity in many-body localized systems," Phys. Rev. B **92**, 104202 (2015).

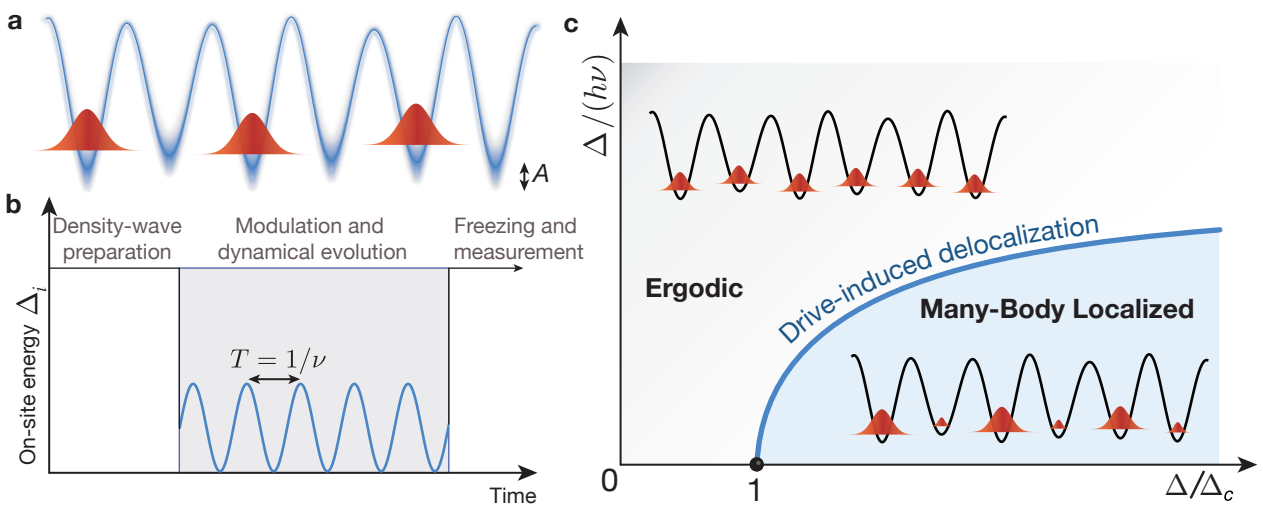
a
A
b
Density-wave preparation
Modulation and dynamical evolution
Freezing and measurement
On-site energy Δ_i
$T = 1/\nu$
Time
c
$\Delta/(h\nu)$
Ergodic
Drive-induced delocalization
Many-Body Localized
0
1
Δ/Δ_c

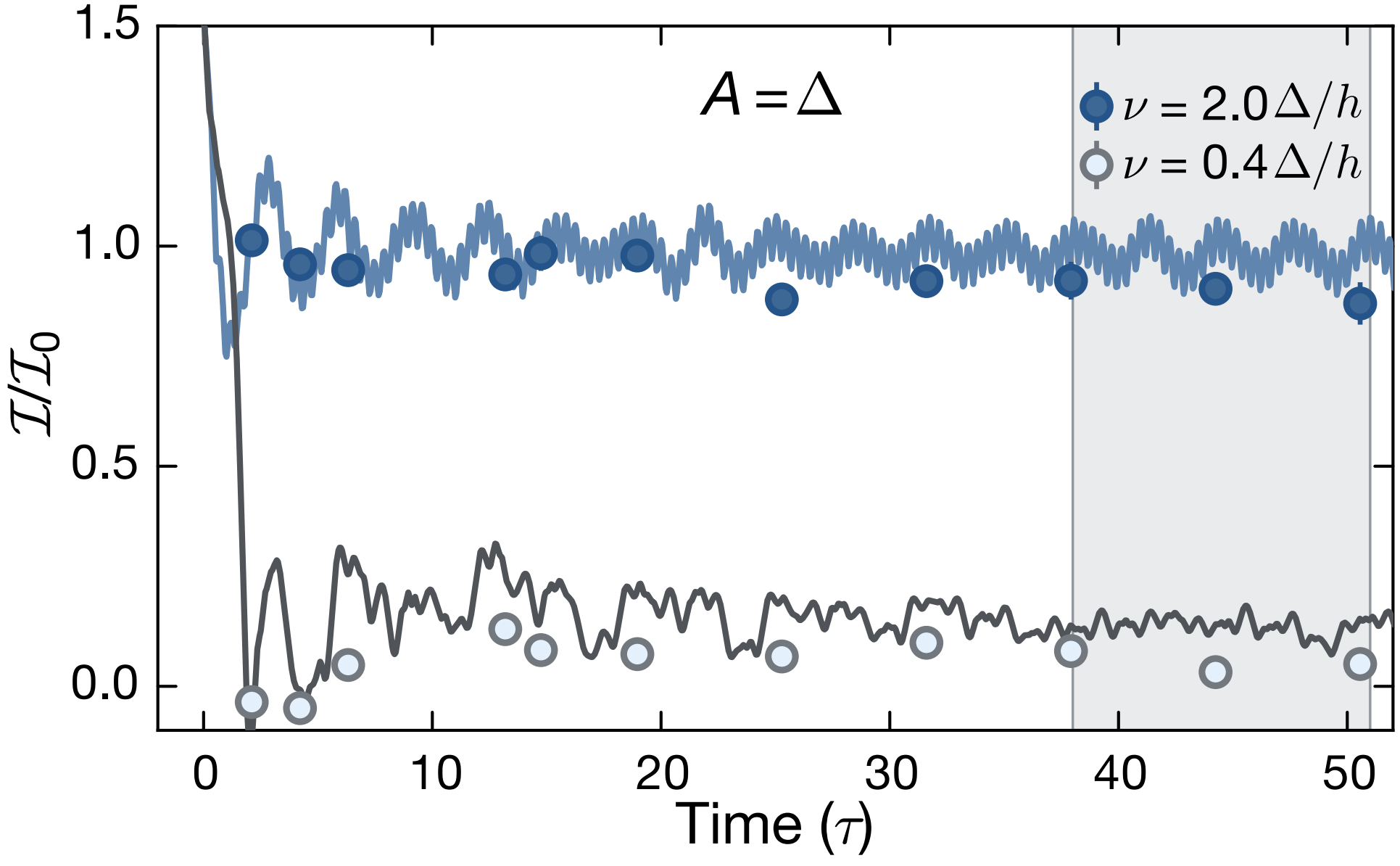
1.5
1.0
0.5
0.0
$\mathcal{I}/\mathcal{I}_0$
$A = \Delta$
$\nu = 2.0\Delta/h$
$\nu = 0.4\Delta/h$
0
10
20
30
40
50
Time (τ)

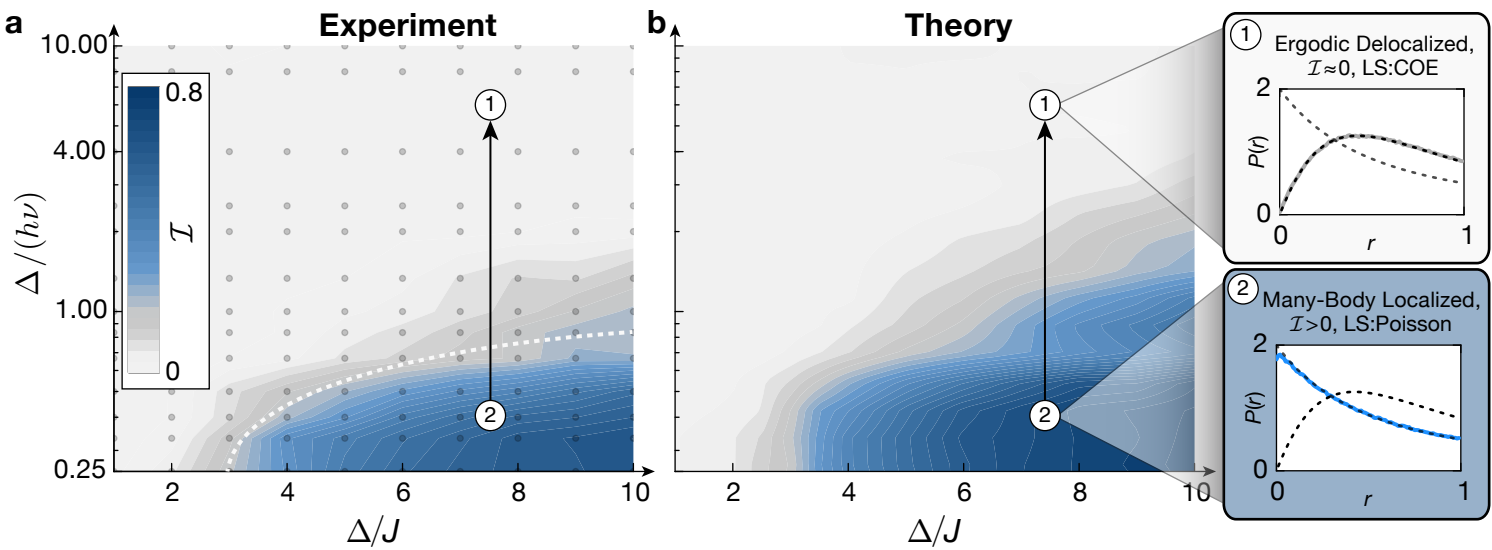
a
Experiment
b
Theory
10.00
4.00
1.00
0.25
$\Delta/(h\nu)$
0.8
0
$\mathcal{I}$
2
4
6
8
10
Δ/J
1
2
① Ergodic Delocalized,
$\mathcal{I}\approx 0$, LS:COE
② Many-Body Localized,
$\mathcal{I}>0$, LS:Poisson
P(r)
r
0
1

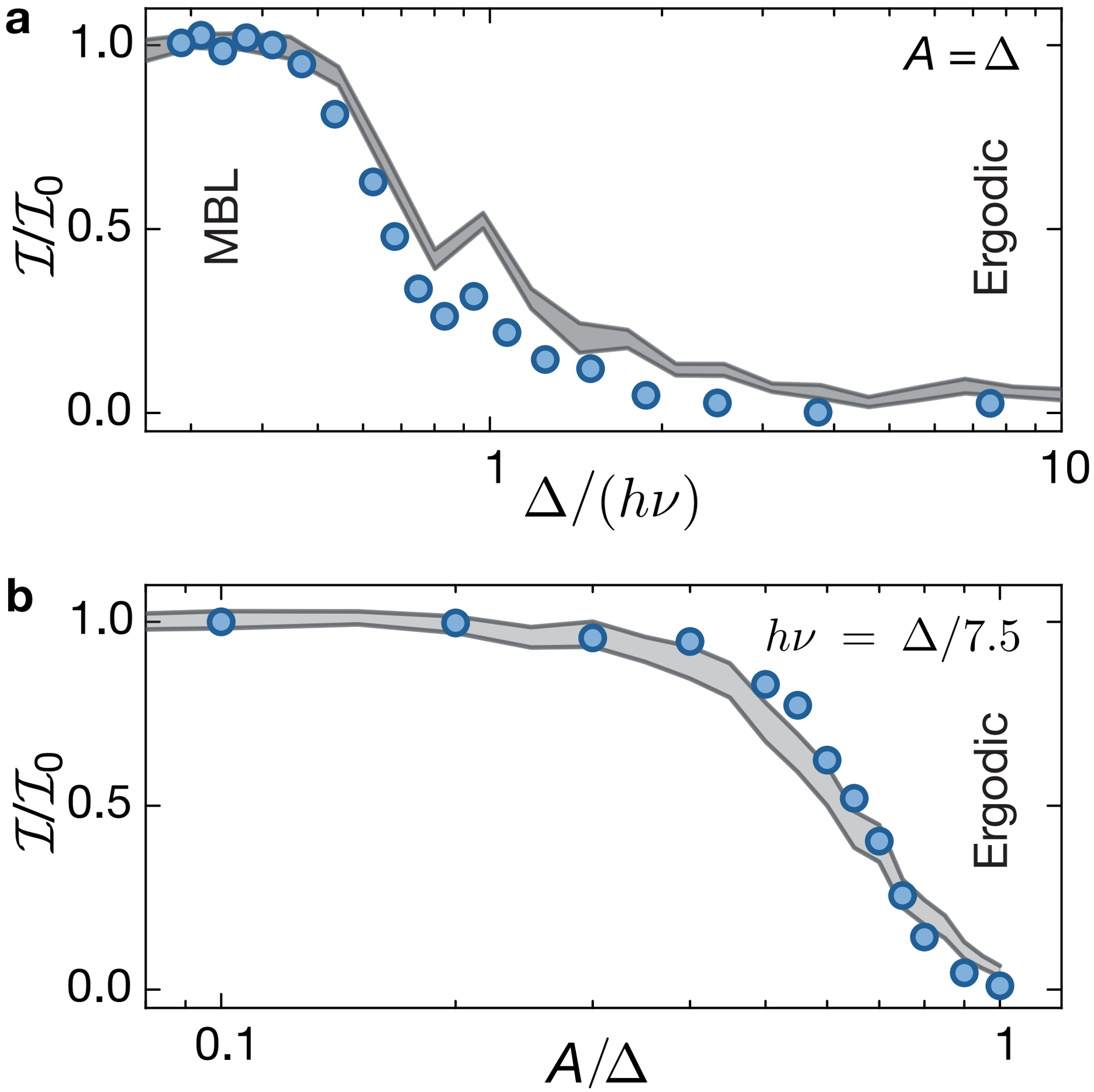
a
1.0
0.5
0.0
$\mathcal{I}/\mathcal{I}_0$
$A = \Delta$
MBL
Ergodic
1
10
$\Delta/(h\nu)$
b
1.0
0.5
0.0
$\mathcal{I}/\mathcal{I}_0$
$h\nu = \Delta/7.5$
Ergodic
0.1
1
A/Δ